

Level-density parameters in superheavy nuclei

A. Rahmatinejad, A. N. Bezbakh, T. M. Shneidman,* G. Adamian, and N. V. Antonenko
Joint Institute for Nuclear Research, Dubna, 141980, Russia

P. Jachimowicz
Institute of Physics, University of Zielona Góra, Szafrana 4a, 65516 Zielona Góra, Poland

M. Kowal†
National Centre for Nuclear Research, Pasteura 7, 02-093 Warsaw, Poland
(Dated: May 19, 2020)

We systematically study the nuclear level densities of superheavy nuclei, including odd systems, using the single-particle energies obtained with the Woods-Saxon potential diagonalization. Minimization over many deformation parameters for the global minima - ground states and the "imaginary water flow" technique on many deformation energy grid for the saddle points, including nonaxial shapes has been applied. The level density parameters are calculated by fitting the obtained results with the standard Fermi gas expression. The total potential energy and shell correction dependencies of the level-density parameter are analyzed and compared at the ground state and saddle point. These parameters are compared with the results of phenomenological expression. As shown, this expression should be modified for the saddle points, especially for small excitation energy. The ratio of the level-density parameter at the saddle point to that at the ground state is shown to be crucial for survival probability of heavy nucleus.

PACS numbers: 21.10.Ma, 21.10.Pc, 24.60.Dr, 24.75.+i

Keywords: microscopic-macroscopic model, fission barrier, level-density parameter, survival probability, superheavy nuclei

I. INTRODUCTION

Considerable progress in the experimental synthesis of new superheavy nuclei has been achieved recently [1, 2] and further experiments on producing heavier elements are planned with the constructed new "superheavy factory" at JINR. The success in production of superheavy nuclei mainly depends on how strongly a hot compound nucleus, created in complete fusion reaction, is opposed to the fission process. Thus, the survival probability, which takes into account the competition between neutron emission and fission, plays an important role in the formation of evaporation residues. The relative importance of these two decay modes mainly depends on the corresponding level densities. To estimate which of the decay processes wins this competition, one should know the level densities at the ground states and at the fission saddle points. Moreover, the height and position of the saddle point are crucial for estimation of survival probability of excited compound nucleus.

To calculate level densities, one can determine all eigenvalues, with their degeneracy, of the nuclear Hamiltonian and then count how many of them are into the energy interval of interest. Because the total number of states exponentially increases with excitation energy above several MeV, the problem becomes treatable only statistically. There are a number of sophisticated combi-

natorial methods to do this, see for example Refs. [3, 4] where the parity, angular momentum, pairing correlations as well as collective enhancements are explicitly treated based on the Gogny interaction. As shown in Ref. [5], there is the general and exact scheme how to calculate the particle-hole level densities for an arbitrary single-particle Hamiltonian taking into account the Pauli exclusion principle. The spin- and parity-dependent shell-model nuclear level densities obtained with the moment method in the proton-neutron formalism is presented in Ref. [6]. Direct microscopic calculation of nuclear level densities in the shell model Monte-Carlo approach is presented in Ref. [7]. Despite this, in practical applications we still must use a number of approximations and assumptions, and even corrections as superfluidity effect or collective rotational and vibrational enhancement.

Ultimately, the most important in practical applications is the empirical level-density parameter a which is studied in this article. One should remember that the level density at the saddle is not the same as that at the ground state. Indeed, the energy available for occupation of the levels at the saddle point is lowered by the difference in the deformation energy between the saddle and ground states. Another reason is that the single-particle levels are distributed differently due to the change of geometrical shape of compound nucleus. It is therefore crucial to find the right saddle point that governs the fission process. To find all saddle points on energy hypercube and then choose the proper one between them is quite a demanding task.

Based on the fact that going from low to higher ener-

*Also at Kazan Federal University, Kazan 420008, Russia

†Electronic address: michal.kowal@ncbj.gov.pl

gies the nuclear system reverts from a paired system to a system of noninteracting fermions, one can successfully describe it with the well-known Fermi-gas model. In this phenomenological model, the pairing effect is taken into account with a constant parameter Δ . In the Fermi-gas model, the average value of the level-density parameter, which establishes the connection between the excitation energy and nuclear temperature, is often assumed to depend linearly on the mass number A [8]. In real situation, the level-density parameter is energy dependent and gradually reaches an asymptotic value with increasing energies above the neutron separation energy. The phenomenological expression has been introduced in Ref. [9] to determine the energy and shell correction dependencies of the level-density parameter.

The main goal of this paper is to combine the state of art methods: imaginary water flow technique on a many deformation space for saddles and multidimensional minimisation for ground states with the statistical approach for calculation of level-density parameters at those extreme (saddles and minima) points. We use the BCS model to calculate the intrinsic level densities of superheavy nuclei with $Z = 112, 114, 116, 117, 118$, and 120. As known, this formalism is successful in description of nuclear quantities such as level density and isomeric ratio [10]. The ratio of the level density parameter at the saddle point to that at the ground state is important to calculate the survival probability of excited heavy nucleus. This ratio will be considered with the energy dependence of neutron emission probability from excited heavy and superheavy nuclei.

II. METHOD OF CALCULATION

We apply a two-step approach. In the first step of our calculation of the level density, using the macroscopic - microscopic (MM) method, we determine all necessary minima and saddle points. The minima are calculated by using multi-dimensional minimization while the saddle points by applying Imaginary Water Flow technique (IWF) on multidimensional energy grids. In the second stage, we use the statistical formalism allowing to estimate the level-density parameters at these extreme points employing the deformed single-particle spectra.

A. Ground states and saddle points

To calculate the potential energy surfaces, the MM method is used. In the frame of this method the microscopic energy is calculated by applying the Strutinski shell and pairing correction method [11] with the single-particle levels obtained after diagonalization of the deformed Woods-Saxon potential [12]. The $n_p = 450$ lowest proton levels and $n_n = 550$ lowest neutron levels from the $N_{max} = 19$ lowest shells of the harmonic oscillator are taken into account in the diagonalization procedure. The

standard values of $\hbar\omega_0 = 41/A^{1/3}$ MeV for the oscillator energy and $\gamma = 1.2\hbar\omega_0$ for the Strutinski smearing parameter, and a six-order correction polynomial are used in the calculation of the shell correction. For the macroscopic part, we use the Yukawa plus exponential model [13] with the parameters specified in Ref. [14]. The deformation dependent Coulomb and surface energies are integrated by using the 64-point Gaussian quadrature.

For nuclear ground states, based on our previous tests and results [15–17], we confined our analysis to axially-symmetric shapes parameterized by spherical harmonics expansion of the nuclear radius truncated at β_{80} :

$$R(\vartheta, \varphi) = cR_0\{1 + \beta_{20}Y_{20} + \beta_{30}Y_{30} + \beta_{40}Y_{40} + \beta_{50}Y_{50} + \beta_{60}Y_{60} + \beta_{70}Y_{70} + \beta_{80}Y_{80}\}, \quad (1)$$

where the dependence of spherical harmonics on φ is suppressed and c is the volume-fixing factor depending on deformation. In this case, the energy is minimized over 7 degrees of freedom specified in (1), by using the conjugate gradient method. To avoid falling into local minima, the minimization is repeated dozens of times for each nucleus, with randomly selected starting deformations. For odd systems, the additional minimization over configurations is performed at every step of the gradient procedure.

Triaxial and mass-asymmetric deformations are included and the IWF method is used for finding the saddles. This allows us to avoid errors inherent in the constrained minimization approach [18–21]. This very efficient technique in the study of fission barriers was first applied in Ref. [22]. To find saddles, the energy for each nucleus is calculated on the 5D deformation grid and then fivefold interpolated in each dimension for the IWF search.

So, in order to find the proper first saddle point we use a five dimensional deformation space, with the expansion of the nuclear radius:

$$R(\vartheta, \varphi) = cR_0\{1 + \beta_{20}Y_{20} + \frac{\beta_{22}}{\sqrt{2}}[Y_{22} + Y_{2-2}] + \beta_{40}Y_{40} + \beta_{60}Y_{60} + \beta_{80}Y_{80}\}, \quad (2)$$

where the quadrupole non-axiality β_{22} is explicitly included. For each nucleus we generate the following 5D grid of deformations:

$$\begin{aligned} \beta_{20} &= 0.00 (0.05) 0.60 \\ \beta_{22} &= 0.00 (0.05) 0.45 \\ \beta_{40} &= -0.20 (0.05) 0.20 \\ \beta_{60} &= -0.10 (0.05) 0.10 \\ \beta_{80} &= -0.10 (0.05) 0.10 \end{aligned} \quad (3)$$

of 29 250 points (nuclear shapes); the numbers in the parentheses specify the grid steps. Additionally, for odd - and odd - odd nuclei, at each grid point we look for low-lying configurations blocked by particles on levels from the 10-th below to the 10-th above the Fermi level. Then,

our primary grid (3) was extended by the fivefold interpolation in all directions. Finally, we obtained the interpolated energy grid of more than 50 million points. To find the first saddles on such a giant grid, we use the IWF method (see e.g. [23, 24]).

B. Level-density parameters

Based on the superconducting formalism [25], the constants (G_N and G_Z) of pairing interaction for neutrons and protons are adjusted to obtain the ground-state pairing gaps (Δ_N and Δ_Z) of the MM method with the following equations:

$$N = \sum_k \left(1 - \frac{\varepsilon_{N,k} - \lambda_N}{E_{N,k}} \tanh \frac{\beta E_{N,k}}{2} \right), \quad (4)$$

$$\frac{2}{G_N} = \sum_k \frac{1}{E_{N,k}} \tanh \frac{\beta E_{N,k}}{2}, \quad (5)$$

for neutrons and,

$$Z = \sum_k \left(1 - \frac{\varepsilon_{Z,k} - \lambda_Z}{E_{Z,k}} \tanh \frac{\beta E_{Z,k}}{2} \right), \quad (6)$$

$$\frac{2}{G_Z} = \sum_k \frac{1}{E_{Z,k}} \tanh \frac{\beta E_{Z,k}}{2}, \quad (7)$$

for protons at zero temperature. The quasiparticle energies $E_{N(Z),k} = \sqrt{(\varepsilon_{N(Z),k} - \lambda_{N(Z)})^2 + \Delta_{N(Z)}^2}$ are calculated using the single-particle energies ($\varepsilon_{N(Z),k}$) of the Woods-Saxon potential. Using the obtained values of the pairing constants, the pairing gaps and chemical potentials ($\lambda_{N(Z)}$) are determined by solving Eqs.(4)–(7) at given temperatures ($T = 1/\beta$). Then, setting the obtained values in the following equations the excitation energies ($U = U_Z + U_N$), entropies ($S = S_Z + S_N$) and intrinsic level densities (ρ) are calculated:

$$E_{Z,N}(T) = \sum_k \varepsilon_k \left(1 - \frac{\varepsilon_k - \lambda_{Z,N}}{E_k} \tanh \frac{\beta E_k}{2} \right) - \frac{\Delta_{Z,N}^2}{G_{Z,N}}, \quad (8)$$

$$U_{Z,N}(T) = E_{Z,N}(T) - E_{Z,N}(0), \quad (9)$$

$$S_{Z,N}(T) = \sum_k \left\{ \ln[1 + \exp(-\beta E_k)] + \frac{\beta E_k}{1 + \exp(\beta E_k)} \right\}, \quad (10)$$

$$\rho = \frac{\exp(S)}{(2\pi)^{\frac{3}{2}} \sqrt{D}}, \quad (11)$$

where D is the determinant of the matrix comprised of the second derivatives of the entropy with respect to β

and $\mu = \beta\lambda$. The calculations were repeated using the single-particle level energies obtained with the Woods-Saxon potential at the saddle point. In the BCS calculations of the saddle point the pairing constants were taken from the ground-state results. Above critical temperature (T_{cr}) the pairing gap vanishes and all thermodynamical quantities revert to those of a noninteracting Fermi system. Generally, larger density of states close to the Fermi surface at the saddle point leads to larger pairing correlation and as a consequence larger value of the critical temperature in comparison to the ground state. In the mass region considered, the critical temperatures for neutrons and protons are up to 0.42 MeV at the ground state, and 0.52 MeV at the saddle point. The corresponding total excitation energies are $U_{cr} \approx 5.14$ MeV at the ground state and $U_{cr} \approx 11.27$ MeV (with respect to the ground state) at the saddle point. Fitting the calculated values of intrinsic level density at an specified excitation energy with the back-shifted Fermi gas expression

$$\rho_{FG}(U) = \frac{\sqrt{\pi}}{12a^{\frac{1}{4}}(U - \Delta)^{\frac{5}{4}}} \exp(2\sqrt{a(U - \Delta)}), \quad (12)$$

one can obtain the level density parameter $a(U)$ as a function of excitation energy. In the calculations, the energy back-shifts are taken as $\Delta = 24/\sqrt{A}$, $12/\sqrt{A}$, and 0 MeV for even-even, odd and odd-odd isotopes, respectively. Energy and shell correction (δE_{sh}) dependencies of the level density parameter can be described with the following phenomenological expression [9]

$$a(A, U) = \tilde{a}(A) \left[1 + \frac{1 - \exp(-(U - \Delta)/E_D)}{U - \Delta} \delta E_{sh} \right], \quad (13)$$

where E_D is known as the damping parameter and indicates how the shell effect in the levelsplgrid density parameter damps with increasing U . We would like to emphasise that we obtain the damping parameter and the asymptotic value \tilde{a} of the level density parameter by analyzing the calculated energy dependent level-density parameter with Eq. (13) for each considered nucleus separately. However, for practical reasons, we also want to stay at the phenomenological level. To do this one can find systematics of \tilde{a} as this value smoothly depends on the mass number, see Ref. [9]

$$\tilde{a} = \alpha A + \beta A^2. \quad (14)$$

The damping parameter, in turn can be approximated as:

$$E_D = A^{1/3}/\gamma_0. \quad (15)$$

Here, α , β , and γ_0 are the parameters providing the best fit of the calculated energy dependent level density parameters in the nuclei considered.

C. Survival probability

Finally, the most important seems to be the use of this formalism to estimate the probability of survival of the

synthesized nucleus. The survival probability of heavy and superheavy nuclei is proportional to the ratio of neutron emission width (Γ_n) to fission width (Γ_f) [26]. This ratio is calculated as:

$$\frac{\Gamma_n}{\Gamma_f} = \frac{gA^{2/3} \int_0^{U-B_n} \varepsilon \rho_{GS}(U - B_n - \varepsilon) d\varepsilon}{K_0 \int_0^{U-B_f} \rho_{SP}(U - B_f - \varepsilon) d\varepsilon}, \quad (16)$$

where g is the neutron intrinsic spin degeneracy, $K_0 \approx 10$ MeV [26] and B_n and B_f are neutron separation energy and fission barrier height, respectively. Here, ρ_{GS} and ρ_{SP} are the level densities calculated at the ground state and saddle point, respectively. Based on the Fermi gas model, the following analytical expression of Γ_n/Γ_f can be obtained [26]

$$\frac{\Gamma_n}{\Gamma_f} = \frac{4A^{2/3} a_f (U - B_n - \Delta_n)}{K_0 a_n \left[2a_f^{1/2} (U - B_f - \Delta_f)^{1/2} - 1 \right]} \times \exp \left[2a_n^{1/2} (U - B_n - \Delta_n)^{1/2} - 2a_f^{1/2} (U - B_f - \Delta_f)^{1/2} \right], \quad (17)$$

where Δ_f and Δ_n are the back-shifts in the Fermi gas level densities at the saddle point and ground state, respectively. Assuming only neutron emission and fission decay channels, the neutron emission probability is written as

$$\frac{\Gamma_n}{\Gamma_{tot}} = \frac{\Gamma_n/\Gamma_f}{1 + \Gamma_n/\Gamma_f}, \quad (18)$$

and strongly affected by the ratio

$$\frac{a_f}{a_n} = \frac{a_{SP}(A, U - B_f)}{a_{GS}(A - 1, U - B_n)}, \quad (19)$$

which should be calculated and discussed for the superheavy nuclei considered.

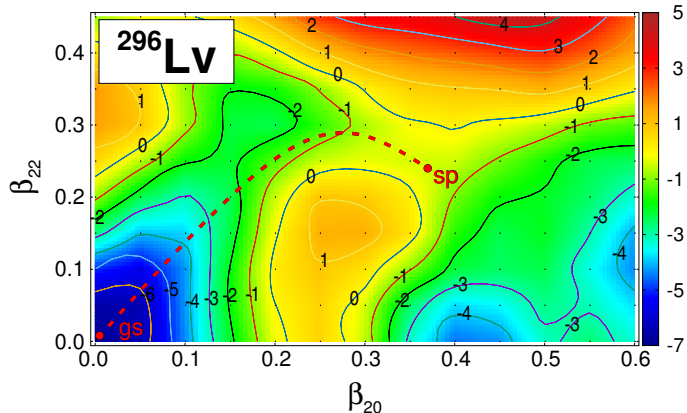


FIG. 1: Potential energy landscape projected into (β_{20}, β_{22}) plane for ^{296}Lv . Possible fission path is shown by dashed line from the ground state (gs) to the saddle point (sp). Energy (in MeV) is calculated relative to the macroscopic energy at the spherical shape.

III. RESULTS AND DISCUSSION

A. Proton and neutron single-particle spectra

As we want to compare the behavior of the level density at saddles in relation to that at the ground state, we start with a description (giving an example) of their determination, which is crucial for further work. As mentioned in Sect. II, the determination of the fission barrier in multidimensional space requires hypercube calculations and application of the IWF technique on it. The potential energy surface for ^{296}Lv , as an example, is shown in Fig. 1 on the $(\beta_{20}; \beta_{22})$ plane obtained by minimizing energy on the five-dimensional grid (3) with respect to $\beta_{40}, \beta_{60}, \beta_{80}$. The landscape modification obtained by including quadrupole nonaxiality deformation β_{22} in (2) is important for the picture of the first saddle points. The strong reduction of axial barrier, by about 2 MeV, due to this effect is clearly seen on the map. One should keep in the mind that the energy mapping in multidimensional space becomes a problem. A reduction of dimension via the minimization over some deformations often leads to an energy surface composed from disconnected patches, corresponding to multiple minima in the auxiliary (those minimized over) dimensions. This is why the real saddle point found with the IWF technique in full deformation space may be located in a slightly different place than the one shown in Fig. 1. Example of fission path starting from nearly spherical ground state and ending on triaxial saddle point is shown in Fig. 1 by red-dashed line. Along the fission path the orders of the Woods-Saxon single-particle levels are shown in Figs. 2 and 3 for protons and neutrons, respectively. The evolution of the Fermi level ($\lambda_{p(n)}$) is traced by black-dotted lines in both cases.

Our calculations show that Eq. (13) for $a(A, U)$ gives a good agreement with the BCS calculations at the ground state, in which the values of the shell corrections are significant. This is fully supported by the single-particle spectra shown in Fig. 2 for protons and in Fig. 3 for neutrons from which one can see the importance of shell effects. First clearly visible is a large energy gap for $Z = 114$ and much smaller, although still distinct for $Z = 120$ at the ground states. This obviously contributes to the significant value of the shell effect in the ground state. When approaching the saddle point the spectrum becomes more complicated with a lot of level crossings. However, it is clear that the single-particle spectrum at the saddle is quite uniform and this is why the shell correction energy is expected to be small.

Even more complicated picture of single-particle states we obtain after diagonalization of deformed Woods-Saxon potential for neutrons. A sufficiently wide energy gap at $N = 184$ is confirmed at the ground state. There is smaller but clear energy gap at $N = 178$. The single-particle spectrum is denser for neutrons than that for protons.

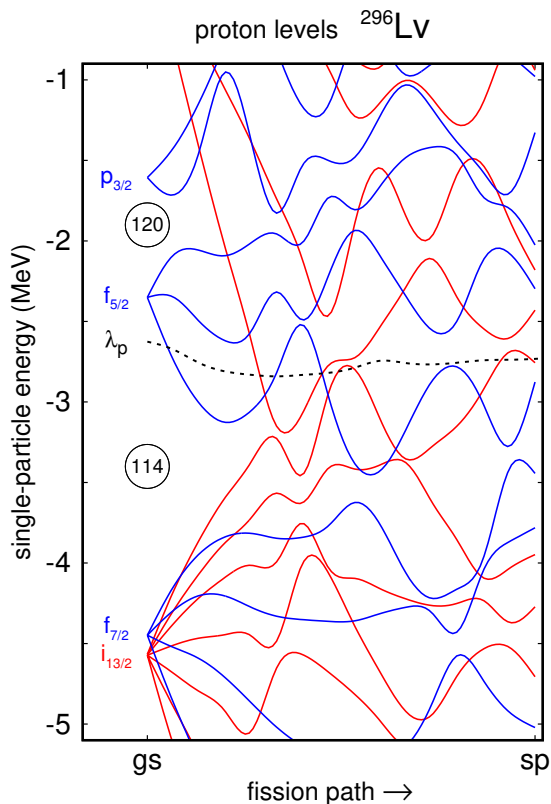


FIG. 2: Proton single-particle spectrum along the fission path for ^{296}Lv (see Fig. 1). The Fermi level is indicated by dotted line.

B. Level-density parameter

The comparisons of energy dependencies of the level-density parameter $a(A, U)$ from the fit of the calculated level densities with Eq. (12) and those obtained from Eq. (13) are presented in Fig. 4 for ^{292}Fl , ^{296}Lv , and $^{300}120$ nuclei. As seen, there is a very good agreement of these dependencies at $U \geq 15$ MeV. Analysing mass number dependence of the asymptotic level density parameters with Eq. (14), we find the coefficients $\alpha = 0.09 \text{ MeV}^{-1}$, $\beta = 2.89 \times 10^{-5} \text{ MeV}^{-1}$ for the ground state (see Fig. 5(a)). These values are close to those obtained in Ref. [27]. Damping parameters calculated independently for every nuclear systems at the ground states are shown in Fig. 7(b). Despite the rather scatter nature of this parameter to use Eq. (13) one can try still to find universal value for E_D . As found, the ground-state damping parameters are in average close to $E_D \approx 15$ MeV. Our results in Fig. 5(b) show that in the nuclei considered the value of E_D can be calculated with Eq. (15) taking $\gamma_0 = 0.423 \text{ MeV}^{-1}$. This value is close to that obtained in Ref. [28] from the analysis of neutron resonance densities and low-lying nuclear levels.

In Fig. 6, the energy dependencies of the saddle-point a calculated for ^{292}Fl , ^{296}Lv , and $^{300}120$ are compared with

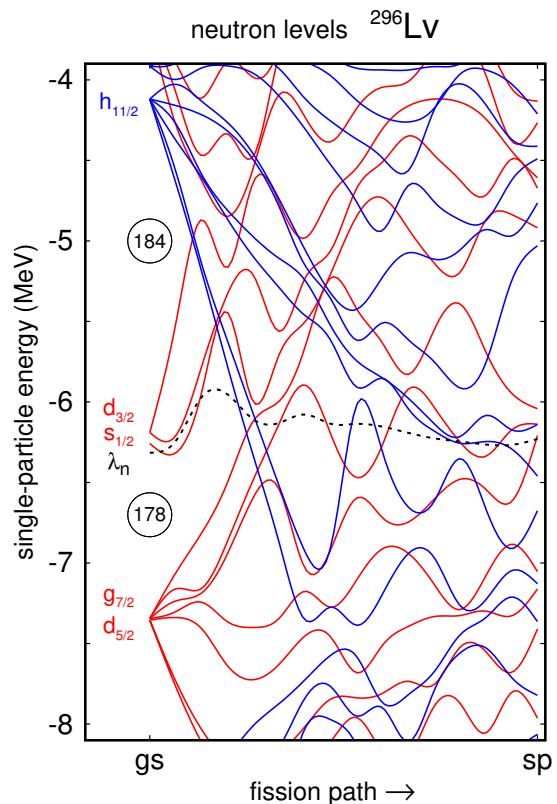


FIG. 3: The same as in Fig. 2, but for the neutron single-particle spectrum.

the phenomenological model (13). At the saddle point, the shell corrections are rather small or even close to zero and, thus, Eq. (13) is unsuitable to describe the calculated values of $a(A, U)$. Replacing the pure shell correction, taken as indicated just from the diagonalization of the deformed Woods-Saxon potential, in Eq. (13) by $(\delta E_{sh} - \Delta_N - \Delta_Z)$, we have much better agreement with the results of direct calculations. We obtain the following coefficients: $\alpha = 0.122 \text{ MeV}^{-1}$ and $\beta = -7.3 \times 10^{-5} \text{ MeV}^{-1}$ in the mass dependence (14) of \tilde{a} . It should be noted that, as in the case of the ground state, we got practically linear dependence of the parameter \tilde{a} with mass number, as β is only of the order of $\sim 10^{-5}$ in both ground and saddle points. Comparison between the values of \tilde{a} at the saddle point with the result of Eq. (14) is shown in Fig. 7(a). Damping parameters calculated independently for every nuclear systems at saddle points are shown in Fig. 7(b). As seen in Fig. 7(b), the saddle-point damping parameters are close to $E_D \approx 17$ MeV for $A < 290$. Though the formal fit results in small value of E_D at the saddle point for $A > 290$, in the calculation of the survival probability one can use larger E_D because the shell effects at the saddle points are small in these nuclei and their damping rate weakly influences the level density parameter in accordance with Eq. (13). Indeed, if the value of $|\delta E_{sh}|$ is small, then the second term in

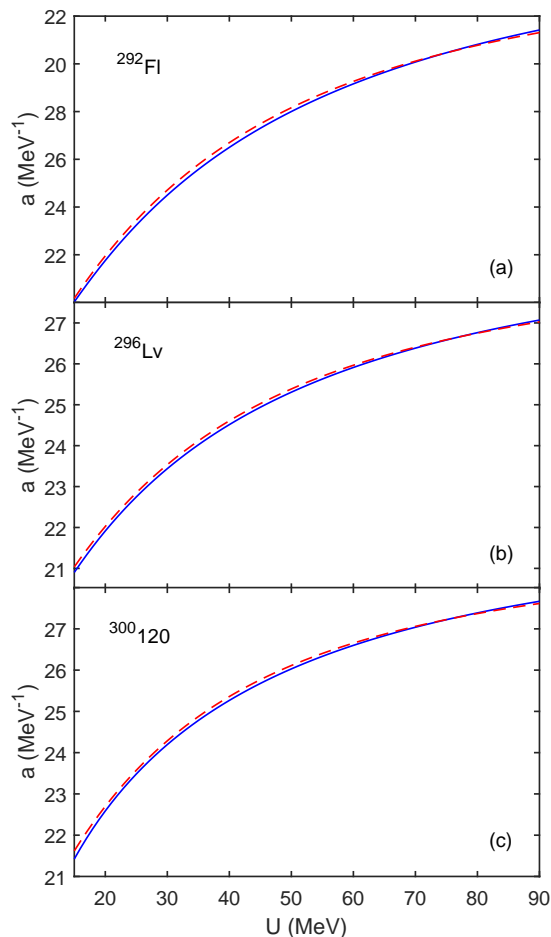


FIG. 4: Comparison of energy dependencies of the ground-state level-density parameters obtained by fitting the calculated level densities (11) with the Fermi-gas expression (12) at the ground state (solid lines) and those obtained with the phenomenological expression (13) (dashed lines) for nuclei ^{292}Fl (a), ^{296}Lv (b), and $^{300}_{120}$ (c).

the parentheses in Eq. (13) is much smaller than unity.

The ratio $a_{SP}(A, U - B_f)/a_{GS}(A, U)$ of the level-density parameter at the saddle point to that at the ground state is shown in Fig. 8(a) for $Z = 114$ isotopic chain at various excitation energies U . The shell effects, which are evident in the a ratios at $U \geq 20$ MeV, decrease at higher energies. In Fig. 8(b), the shell effects ($U = 0$) are presented at the ground state (solid line) and saddle point (dashed line) for various Fl isotopes. Though the shell effects at the ground state are of most importance, they can not be disregarded at the saddle point. So, the *topographic theorem* [29], that the shell effect disappear at the saddle point and the fission barrier is just equal to the shell energy as the nucleus possesses at the ground state, is only approximately valid for superheavy nuclei.

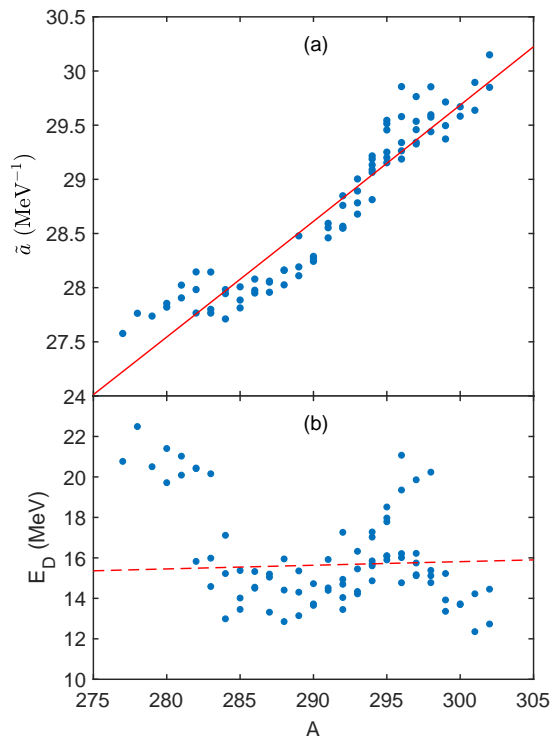


FIG. 5: (a) Mass number dependence of the asymptotic ground-state level-density parameter $\tilde{a}(A)$ obtained with the phenomenological expression (13) (symbols). The fit of $\tilde{a}(A)$ with Eq. (14) is shown by solid line. (b) The corresponding damping parameters (symbols) in Eq. (13) are approximated by $E_D = A^{1/3}/0.423$ (dashed line).

C. Fission and neutron emission probabilities

Because the statistical approach is used here, the details of the fission path variability between extremes are not that important. Only the thresholds that prohibit specific decay are required: the separation energy with the mass of daughter nucleus for decay via neutron emissions and the height of fission barrier.

To validate our calculations of the level densities, first we compare the calculated fission probabilities Γ_f/Γ_{tot} for ^{236}U and ^{240}Pu with the available experimental data. In Fig. 9, the energy dependence of Γ_f/Γ_{tot} calculated with Eqs. (16)–(18) is shown for ^{236}U and ^{240}Pu together with the experimental data from Ref. [30]. In this calculation the values of B_n are obtained from the experimental binding energies and the B_f values are taken as the experimental highest fission saddles, i.e., the first saddle for ^{240}Pu [31], and second saddle for ^{236}U [28]. As seen, the expression (17) gives close results to those of the numerical calculations with Eq. (16). A good agreement with the empirical values seen in Fig. 9 gives us a confidence for the reliable predictions of fission and neutron emission probabilities in the region of heavy nuclei. The values of B_n and B_f calculated in Ref. [24] result

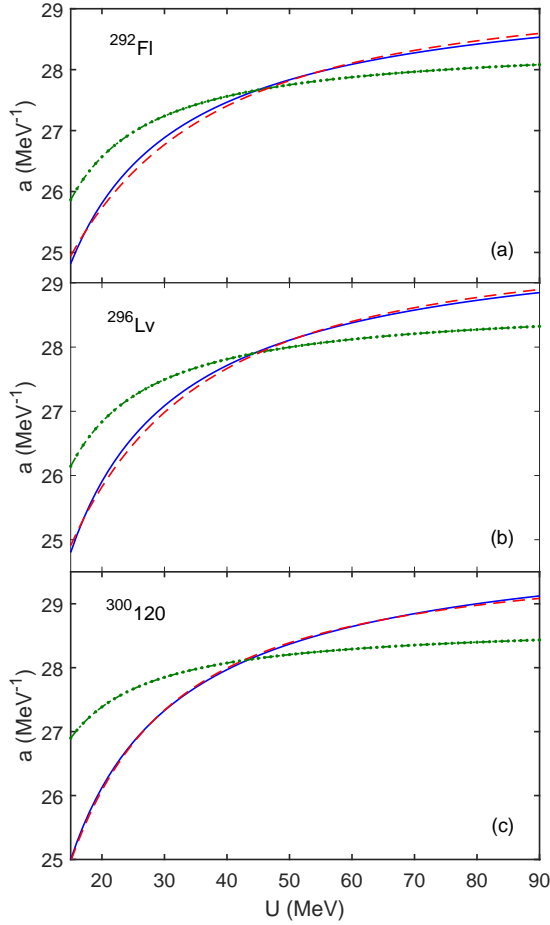


FIG. 6: The same as in Fig. 4, but for the saddle point. The calculated values of a (solid lines) are compared with those from the phenomenological expression (13) with (dashed lines) and without (dash-dotted lines) replacement of the shell correction δE_{sh} by $\delta E_{sh} - \Delta_Z - \Delta_N$.

in Γ_f/Γ_{tot} values which are less within the factor of 2, but just as dependent on energy. At $U > 25$ MeV, the difference is about 10–20%.

In the spirit of canonical Transition-State Theory (TST) [32] the probability ratio for two selected decay types (transitions) is proportional to the number of states available for each of them in the appropriate energy range (saturating total available energy). What means that the excitation energy dependence of Γ_n/Γ_f is strongly affected by the difference between the fission barrier height and neutron binding energy, see schematic Fig. 10.5 in [33] or fig. 9 in [35]. Application of TST in practice one can found e.g in [34–37]. As seen from Eq. (16), at $a_f \approx a_n$ an increasing Γ_n/Γ_f with the excitation energy is expected at $(B_f + \Delta_f) - (B_n + \Delta_n) < 0$, and opposite trend is expected at $(B_f + \Delta_f) - (B_n + \Delta_n) > 0$. However, our calculations show that in the nuclei considered, the a_f values are in average $\sim 10 - 30\%$ larger than a_n . Because of the exponential nature of the survival proba-

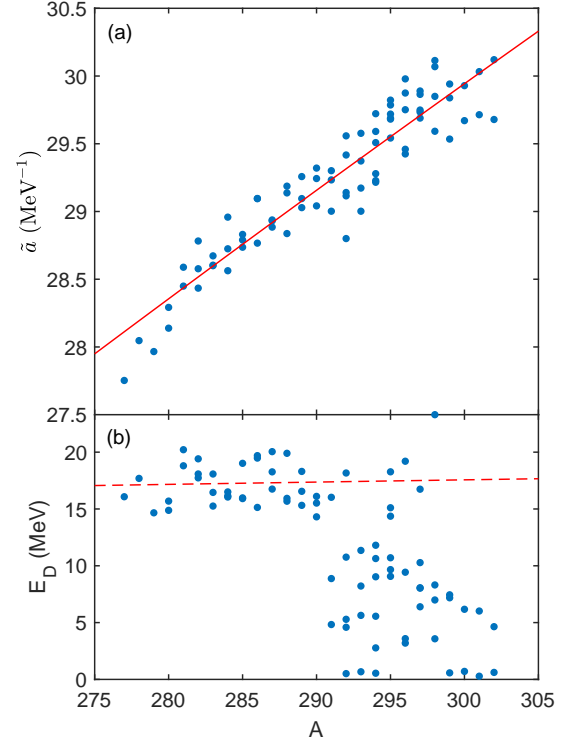


FIG. 7: The same as in Fig. 5, but for the asymptotic saddle-point level-density parameter $\tilde{a}(A)$ and the saddle-point damping parameter E_D . Here, the damping parameters are approximated by $E_D = A^{1/3}/0.381$ (dashed line) for $A < 290$.

bility (17), the ratio of a_f/a_n strongly affects the Γ_n/Γ_f . The calculated ratios a_f/a_n for $Z = 117$ and $Z = 120$ isotopic chains are shown in Fig. 10 for various excitation energies, together with the corresponding phenomenological results obtained with Eq. (13). As seen, the shell and pairing effects decrease with excitation energy and ratios a_f/a_n reach asymptotic values equal more or less 1.1. As consequences of disappearance of quantum effects the visible strong staggering of a_f/a_n weakly significantly with excitation. One can also see that the approximate formula (Eq. (13)) works very well in the whole range of excitation energy for all considered nuclei.

The dependence of a_f/a_n on excitation energy for: ^{284}Fl (green solid line); ^{288}Fl (red dot-dashed line) ^{292}Fl (blue dashed line) isotopes is shown in Fig. 11. In all presented Fl cases a_f/a_n values clearly deviate from 1, for example for ^{284}Fl at maximum is about 1.35. The course of variability of this ratio as a function of excitation energy is similar in all three flerovium nuclei. At first it grows quite quickly to reach a maximum of about 20 MeV and then slowly falls down. Only for very high excitation energies the curves saturate to an asymptotic value of about 1.1

In Fig. 12, the energy dependence of neutron emission probability is shown for ^{278}Cn , ^{294}Og , and $^{296,298}\text{120}$. As follows from the expression (17), the general in-

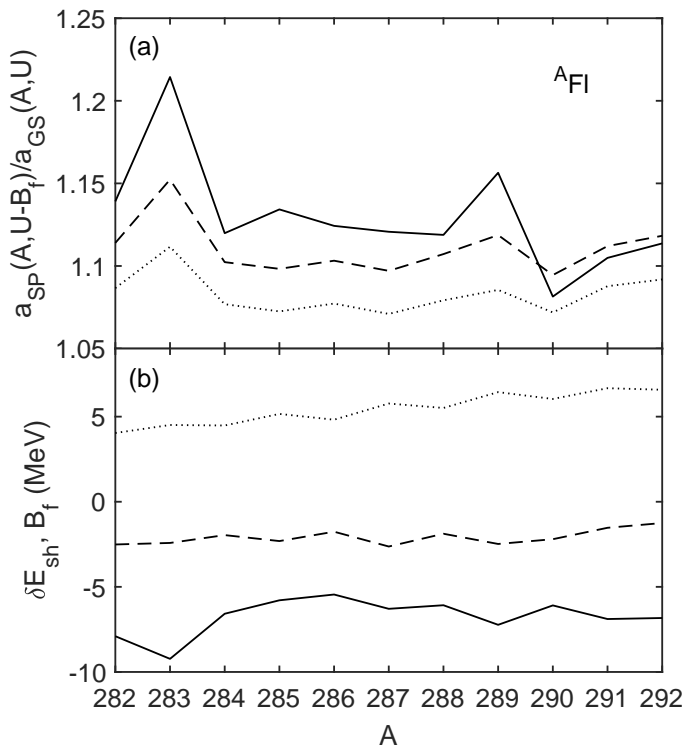


FIG. 8: For ${}^A\text{Fl}$ isotopes, (a) the ratios of the level density parameters at the saddle point and ground state are shown at the excitation energies 20 MeV (solid line), 40 MeV (dashed line), and 60 MeV (dotted line). At the saddle point the excitation energy is decreased by the high B_f of the fission barrier. (b) The values of shell corrections at the ground state (solid line) and the ones at the saddle point (dashed line), and the heights of fission barriers (dotted line) are presented as functions of mass number A at zero excitation energy.

crease of Γ_n/Γ_{tot} with the excitation energy for ${}^{278}\text{Cn}$ and ${}^{296,298}120$ is due to positive values of the derivative of the exponential part $\sqrt{a_n/(U-B_n-\Delta_n)} - \sqrt{a_f/(U-B_f-\Delta_f)} > 0$. Similarly, the condition $\sqrt{a_n/(U-B_n-\Delta_n)} - \sqrt{a_f/(U-B_f-\Delta_f)} < 0$ for ${}^{294}\text{Og}$ (Fig. 12(b)) nucleus leads to a decrease of Γ_n/Γ_{tot} with increasing excitation energy. These exact numerical results are shown in Fig. 12 by solid blue lines. Note, that depending on the superheavy system the scale of Γ_n/Γ_{tot} is different. The local variations seen in Γ_n/Γ_{tot} curves at lower energies may be caused by already discusses strong shell and pairing effects in a_f/a_n . This study proves how important and even decisive is the role of energy dependent level-density parameters at the saddle point and ground state. We have shown in The phenomenological expression (13) seems to be suitable for Eq. (17) to describe the energy dependence of Γ_n/Γ_{tot} . Results of these approximate calculations are shown by red dashed lines in Fig. 12. Only, for $Z=120$ both results vary noticeably for very large excitation energy values, which however, are not important to us here.

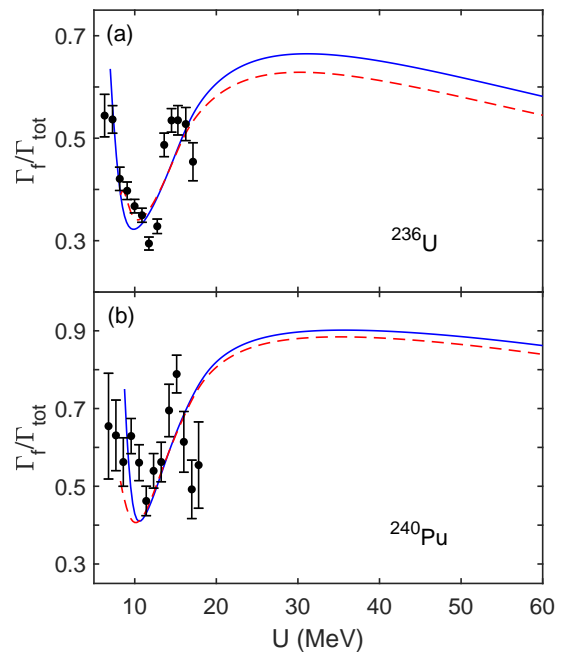


FIG. 9: The dependence of fission probability Γ_f/Γ_{tot} on excitation energy for the fissioning nuclei ${}^{236}\text{U}$ (a), and ${}^{240}\text{Pu}$ (b). The results obtained with Eq. (16) (blue solid line) and analytical expression (17) (red dashed line) are compared with the experimental data (symbols) from Ref. [30].

IV. CONCLUSIONS

Since, the nuclear level density is of special importance for the cross sections calculations and nuclear structure studies in general, we devoted this article to this quantity. It takes on special significance for super-heavy nuclei in which we are dealing with extremely low probabilities of their production. The level-density parameter was evaluated here by fitting of obtained numerical and exact results to the well known Fermi gas expression. The single-particle energies were calculated within the microscopic-macroscopic model based on the diagonalization of the deformed single-particle Woods-Saxon potential. Yukawa-plus exponential model for macroscopic energy calculation has been used. We carried out our analysis not only for the ground states but also for the saddle points, what's new in these kinds of calculations. The energy and shell correction dependencies of the level-density parameter of superheavy nuclei at these extremes were studied and compared with the well-known Ignatyuk expression.

The following conclusions can be drawn:

i) We have shown that phenomenological approach based on Ignatyuk formula agrees well when one calculated energy dependence of the level-density parameter at the ground states and strongly disagree, particularly for small excitation energies, at the saddle point configurations. Thus, Eq. (13) can not be safely used for the

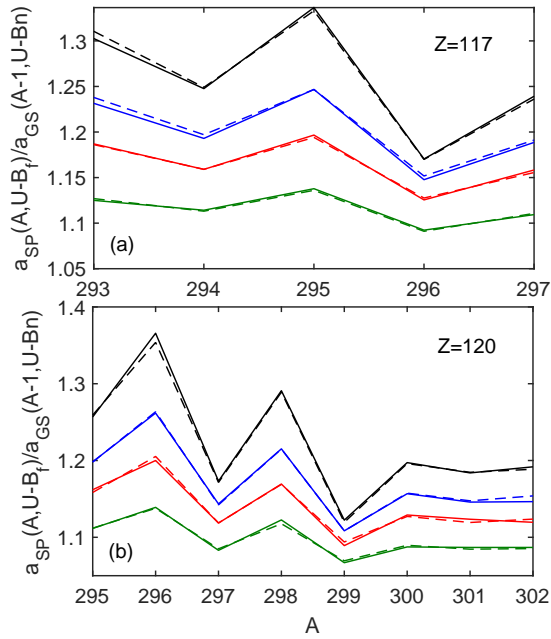


FIG. 10: For $Z = 117$ (a) and $Z = 120$ (b) isotopic chains, the ratios of the level density parameter of the mother nucleus at the saddle point to that of the daughter nucleus after neutron separation at the ground state at $U = 25$ (solid black line), 35 (solid blue line), 45 (solid red line), and 65 MeV (solid green line). The corresponding phenomenological results of Eq. (13) are shown by dashed lines.

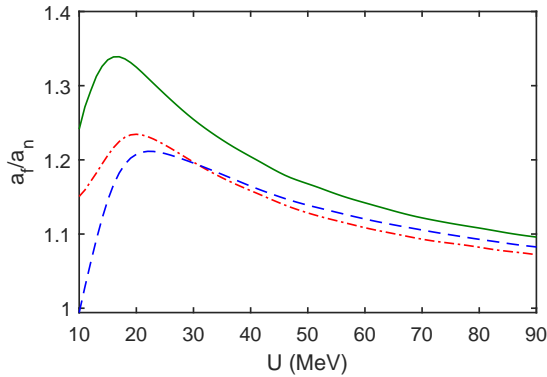


FIG. 11: The dependencies of a_f/a_n (19) on excitation energy for ^{284}Fl (green solid line), ^{288}Fl (red dot-dashed line), and ^{292}Fl (blue dashed line).

saddle at low excitation energies.

ii) Investigated, here the ratio of the level-density parameter at the saddle point to that at the ground state which is a very important factor in evaluation of the probability of fission in comparison to the probability of neutron emissions is far from unity, especially for not to hot nuclear systems.

iii) As shown, the topographic theorem can be applied with some caution to nuclei having a substantial saddle

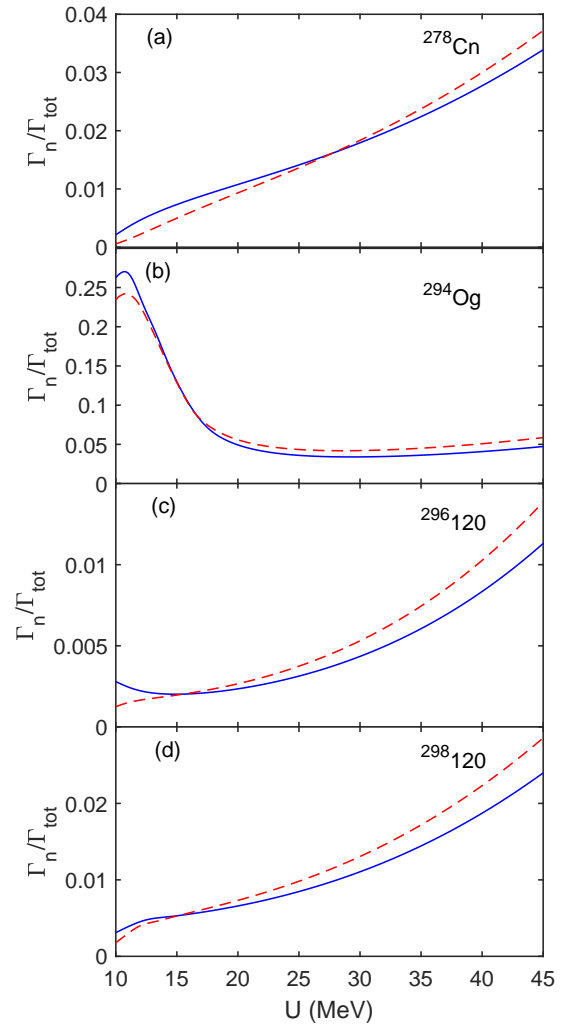


FIG. 12: The dependence of neutron emission probability on excitation energy for ^{278}Cn (a), ^{294}Og (b), $^{296}_{120}$ (c), and $^{298}_{120}$ (d). The increasing trend for ^{278}Cn and $^{296,298}_{120}$ nuclei and decreasing trend for ^{294}Og nucleus are in agreement with the positive or negative sign of derivative of exponential part in (17). Numerical calculations are shown by blue solid lines and the results of expression (17) are depicted by red dashed lines.

point shell correction.

iv) We also note a substantial difference in average level-density parameters between mother nucleus at saddle point and daughter nucleus after neutron emission with expressive staggering effect visible at the same time. Having nuclear level densities at saddles and ground states one can directly/numerically evaluate competition between neutron emission and fission. Numerically determined damping parameters have a stronger effect on the saddle compared to the ground state.

With obtained Γ_n/Γ_{tot} one can calculate the survival probabilities of excited superheavy nuclei without involving any free parameters. Indeed the binding energies, fission thresholds, shells corrections and finally level den-

sities calculated on the same basis are quite important.

ACKNOWLEDGEMENTS

M. K. was co-financed by the National Science Centre under Contract No. UMO-2013/08/M/ST2/00257 (LEA

COPIGAL). This work was partly supported by RFBR (17-52-12015, 20-02-00176) and DFG (Le439/6-1). We are grateful to the Polish-JINR cooperation program for its support. T.M.S. acknowledges Russian Government Subsidy Program of the Competitive Growth of Kazan Federal University.

-
- [1] Yu. Ts. Oganessian and V. K. Utyonkov, *Nucl. Phys. A* **944**, 62 (2015).
- [2] Yu. Ts. Oganessian and K. P. Rykaczewski *Physics Today* **68**, 8, 32 (2015); doi: 10.1063/PT.3.2880
- [3] S. Hilaire, J.P. Delaroche, and M. Girod, *Eur. Phys. J. A* **12**, 169184 (2001).
- [4] S. Goriely, S. Hilaire, and A. J. Koning, *Phys. Rev. C* **78**, 064307 (2008).
- [5] A.H. Blin *et al.*, *Nucl. Phys. A* **456**, 109 (1986).
- [6] R. A. Senkov and M. Horoi, *Phys. Rev. C* **82**, 024304 (2010).
- [7] Y. Alhassid, M. Bonett-Matiz, S. Liu, and H. Nakada *Phys. Rev. C* **92**, 024307 (2015).
- [8] Yu. V. Sokolov, *Level densities of atomic nuclei* (Energoizdat, Moscow, 1990).
- [9] A. B. Ignatyuk, G. N. Smirenkin, and A. S. Tishin *Yad. Fiz.* **21**, 485 (1975).
- [10] P. Decowski, W. Grochulski, A. Marcinkowski, K. Siwek, and Z. Wilhelmi, *Nucl. Phys. A* **110**, 129 (1968).
- [11] V. M. Strutinski, *Sov. J. Nucl. Phys.* **3**, 449 (1966), *Nucl. Phys. A* **95**, 420 (1967).
- [12] S. Ćwiok, J. Dudek, W. Nazarewicz, J. Skalski, and T. Werner, *Comput. Phys. Commun.* **46**, 379 (1987).
- [13] H. J. Krappe, J. R. Nix, and A. J. Sierk, *Phys. Rev. C* **20**, 992 (1979).
- [14] I. Muntian, Z. Patyk, and A. Sobiczewski, *Acta Phys. Pol. B* **32**, 691 (2001).
- [15] M. Kowal, P. Jachimowicz, and A. Sobiczewski, *Phys. Rev. C* **82**, 014303 (2010).
- [16] P. Jachimowicz, M. Kowal, and J. Skalski, *Phys. Rev. C* **89**, 024304 (2014).
- [17] P. Jachimowicz, M. Kowal, and J. Skalski, *Phys. Rev. C* **95**, 034329 (2017).
- [18] W. D. Myers, and W. J. Swiatecki, *Nucl. Phys. A* **601**, 141 (1996).
- [19] P. Möller and A. Iwamoto, *Phys. Rev. C* **61**, 047602 (2000).
- [20] P. Möller *et al.*, *Phys. Rev. C* **79**, 064304 (2009).
- [21] P. Jachimowicz, M. Kowal, and J. Skalski, *Phys. Rev. C* **85**, 034305 (2012).
- [22] A. Mamdouh, J. M. Pearson, M. Rayet, and F. Tondeur, *Nucl. Phys. A* **644**, 389 (1998).
- [23] P. Jachimowicz, M. Kowal, and J. Skalski, *Phys. Rev. C* **95**, 014303 (2017).
- [24] P. Jachimowicz, M. Kowal, and J. Skalski, *Phys. Rev. C* **101**, 014311 (2020).
- [25] G.D. Adeev and P.A. Cherdantsev, *Yad. Fiz.* **21**, 491 (1975).
- [26] R. Vandenbosch and J. R. Huizenga, *Nuclear fission*, (Academic Press, New York, 1973).
- [27] A. N. Bezbakh, T. M. Shneidman, G. G. Adamian, and N. V. Antonenko, *Eur. Phys. J. A* **6**, 50 (2014).
- [28] R. Capote *et al.*, *Nuclear Data Sheets* **110**, 3107 (2009).
- [29] W. J. Swiatecki, *Phys. Rev. C* **100**, 917 (1955).
- [30] E. Cheifetz, H. C. Britt, and J. B. Wilhelmy *Phys. Rev. C* **24**, 519 (1981).
- [31] G. N. Smirenkin, IAEA Report No. INDC(CCP)-359, Vienna, 1993 (unpublished).
- [32] P. Hänggi, P. Talkner, M. Borkovec, *Reaction-rate theory: fifty years after Kramers.*, *Rev. Mod. Phys.*, **62**, (1990).
- [33] P. Fröbrich and R. Lipperheide, *Theory of Nuclear Reactions.*, Oxford University Press Inc., New York, ISBN 0 19 853783 2, (1996).
- [34] W. J. Swiatecki, K. Siwek-Wilczyńska, J. Wilczyński, *Acta Phys. Pol. B* **34**, (2003).
- [35] W. J. Swiatecki, K. Siwek-Wilczyńska, J. Wilczyński, *Phys. Rev. C* **71**, 014602 (2005).
- [36] K. Siwek-Wilczyńska, T. Cap, M. Kowal, A. Sobiczewski, and J. Wilczyński, *Phys. Rev. C* **86**, 014611 (2012).
- [37] K. Siwek-Wilczyńska, T. Cap, M. Kowal, *Phys. Rev. C* **99**, 054603 (2019).